

Multiexponential Electronic Spin Relaxation and Redfield's Limit in Gd(III) Complexes in Solution: Consequences for $^{17}\text{O}/^1\text{H}$ NMR and EPR Simultaneous Analysis

Alain Borel, Fabrice Yerly, Lothar Helm, and André E. Merbach*

Contribution from the Institut de Chimie Moléculaire et Biologique, Ecole Polytechnique Fédérale de Lausanne, EPFL-BCH, CH-1015 Lausanne, Switzerland

Received August 23, 2001

Abstract: Multiple experiments (^{17}O NMR, ^1H NMR, and EPR) have been performed in the past to understand the microscopic parameters that control the magnetic relaxation rate enhancement induced by paramagnetic molecules on neighboring water protons, the so-called relaxivity. The generally accepted theories of the electron spin relaxation of $S = 7/2$ ions such as Gd^{3+} (Solomon–Bloembergen–Morgan or simplified Hudson–Lewis) are unsatisfactory for a simultaneous analysis. Recently, an improved theory, where the electron spin relaxation is due to the combination of a static (thus explicitly linked to the molecular structure) and a dynamic zero field splitting, has been developed and tested on experimental EPR data. The model has also been extended beyond the electronic Redfield limit using Monte Carlo simulations. Using the aqua ion $[\text{Gd}(\text{H}_2\text{O})_9]^{3+}$ as a test case, we present here the first simultaneous analysis of ^{17}O NMR, ^1H NMR, and EPR relaxation data using this rigorous approach of the electron spin relaxation. We discuss the physical meaning of the calculated parameters. The consequences on future experiments are also considered, especially regarding the analysis of nuclear magnetic relaxation dispersion (NMRD) profiles in the study of Gd^{3+} complexes.

Introduction

Paramagnetic Gd^{3+} complexes are widely used as contrast agents in medical magnetic resonance imaging (MRI) due to the enhancement of the relaxation rate of the neighboring protons that they induce.^{1,2} This enhancement, called *relaxivity*, is a consequence of the dipolar coupling between the proton nuclear spin and the electronic spin of the metal ion. Among other factors, relaxivity is determined by (1) the rotational correlation time of the complex τ_R , (2) the water residence time τ_m in the first coordination shell, and (3) the electronic spin relaxation times T_{1e} and T_{2e} . While (1) and (2) are rather well understood,^{1,2} there is still room for improvement when it comes to the theory of electronic spin relaxation of Gd^{3+} complexes relevant for MRI.^{3–6} The influence of the electronic spin relaxation on the

relaxivity, which may be quite important in some cases,⁷ is essentially governed by the decay of the electronic spin magnetization in the direction parallel to the external field. This decay is described by the longitudinal electronic relaxation time T_{1e} of the Gd^{3+} complexes which is too short to be directly measurable by the presently available techniques. Nevertheless, the investigation of the decay of the electronic spin magnetization perpendicular to the external field, usually characterized by a transverse electronic relaxation time T_{2e} , allows an estimation of T_{1e} within the framework of a given model of the electronic relaxation. For a reasonable prediction of T_{1e} , we need to find a model which correctly describes the underlying physics. Consequently, the past few years have witnessed a considerable interest for new studies, both experimental and theoretical, on this particular subject.

Proposed thirty years ago by Hudson and Lewis,⁸ the basic theory of the EPR line shape of Gd^{3+} complexes uses a transient zero-field splitting as the main relaxation mechanism. The transverse electronic spin relaxation cannot be described by a single T_{2e} ; four different relaxation times are necessary as the experimental spectrum results from a superposition of four transitions with different intensities. To simplify this theory, Powell et al.³ proposed empirical formulas to describe both the transverse and longitudinal relaxation times, which they later applied in a unified model to simultaneously interpret ^{17}O NMR,

* To whom correspondence should be addressed. Fax: +41-21-692 38 75. E-mail: andre.merbach@epfl.ch.

- (1) Caravan, P.; Ellison, J. J.; McMurry, T. J.; Lauffer, R. B. *Chem. Rev.* **1999**, *99*, 2293–2352.
- (2) Merbach, A. E.; Tóth, É. *The Chemistry of Contrast Agents in Medical Magnetic Resonance Imaging*; John Wiley & Sons, Ltd: Chichester, UK, 2001.
- (3) Powell, D. H.; Merbach, A. E.; Gonzalez, G.; Brücher, E.; Micskei, K.; Ottaviani, M. F.; Köhler, K.; von Zelewsky, A.; Grinberg, O. Y.; Lebedev, Y. S. *Helv. Chim. Acta* **1993**, *76*, 2129–2146.
- (4) Powell, D. H.; Ni Dubhghaill, O. M.; Pubanz, D.; Helm, L.; Lebedev, Y. S.; Schlaepfer, W.; Merbach, A. E. *J. Am. Chem. Soc.* **1996**, *118*, 9333–9346.
- (5) Clarkson, R. B.; Smirnov, A. I.; Smirnova, T. I.; Kang, H.; Belford, R. L.; Earle, K.; Freed, J. H. *Mol. Phys.* **1998**, *96*, 1325–1332.
- (6) Borel, A.; Tóth, É.; Helm, L.; Jánosy, A.; Merbach, A. E. *Phys. Chem. Chem. Phys.* **2000**, *2*, 1311–1318.

(7) Borel, A.; Helm, L.; Merbach, A. E. *Chem. Eur. J.* **2001**, *7*, 600–610.

(8) Hudson, A.; Lewis, J. W. E. *Trans. Faraday Soc.* **1970**, *66*, 1297–1301.

¹H NMR, and EPR.^{4,9} However, even with the addition of a spin rotation relaxation mechanism, the obtained results were in a generally poor agreement with the experimental EPR data. More recent approaches also account for the dynamic frequency shift, which is a small displacement in the transition frequencies, often neglected. Several theoretical treatments of this effect were proposed (see, for example, Poupko,¹⁰ Strandberg,¹¹ and Clarkson^{5,12}). Unfortunately, the experimental data reported to support these theories were scarce.

The recent EPR experiments performed in this lab on [Gd(H₂O)₈]³⁺ and [Gd(DOTA)(H₂O)]⁻ at various temperatures and field strengths⁶ represent a rich collection of full spectra including peak-to-peak distances supplemented with dynamic frequency shifts. We first interpreted our data with the help of Poupko's approach of the model of the crystal field modulation in the framework of Redfield's relaxation theory.¹³ This analysis, performed for the first time over such a wide temperature and frequency range, showed the shortcomings of the model. As in the work of Powell et al.,⁴ a spin rotation mechanism had to be introduced to obtain a satisfactory fit of the data.

Very recently, Rast et al.^{14–16} developed a refined model of the electronic relaxation of the *S* states of metal ion complexes in solutions. This refined treatment now includes the contribution of the static crystal field surrounding the Gd³⁺ ion caused by its modulation by the rotation of the whole complex, besides a part due to the usual transient crystal zero-field splitting (ZFS) caused by vibration, intramolecular rearrangement, and collision with surrounding solvent molecules. A good agreement with the measured peak-to-peak distances was obtained for [Gd(H₂O)₈]³⁺, [Gd(DTPA)(H₂O)]²⁻, and [Gd(DTPA-BMA)(H₂O)] complexes over wide ranges of magnetic fields and temperatures. The final refinement of this theory, including a rigorous calculation of the EPR line shape, including dynamic frequency shifts and instrumental factors such as spectrum phasing, was successfully applied to the analysis of multiple frequency and temperature spectra of [Gd(H₂O)₈]³⁺ and [Gd(DOTA)(H₂O)]²⁻.¹⁶ In the framework of this new model, and contrary to previous works,^{6,17} it was not necessary to include the spin rotation mechanism in the interpretation of the measurements as this effect is expected to be very weak for molecules larger than a few atoms.^{18,19} The above model was also successful for describing the proton NMRD behavior of probe solutes such as the tetramethylammonium N(CH₃)₄⁺ ions of well-known spatial dynamics with respect to the [Gd(H₂O)₈]³⁺ complex, without additional fitting parameters.²⁰

However, this new model, as well as most of the previous approaches to this problem, was developed in the framework

of the Redfield relaxation theory^{13,21} describing the time dependence of the correlation functions of the spin system components. This theory has essentially two limitations. Denoting by ω_0 the unperturbed Zeeman angular frequency and by H_1 the time-dependent perturbing Hamiltonian inducing electronic transitions between the Zeeman levels, these limitations are $|H_1|\tau_c \ll 1$ and $|H_1|^2\tau_c \ll \omega_0$, where τ_c is the correlation time of the fluctuating term H_1 . The first condition can be violated when we consider large complexes. When the relevant time τ_c is the rotational correlation time of the complex, its inverse which is the rotational diffusion constant D_R can reach values of the same order as H_1 , especially in the low-temperature region where D_R decreases. The second condition corresponds to the secular approximation²² and is barely satisfied when experiments are performed at low fields, mainly for large complexes and at temperatures just above 0 °C.

To overcome these problems, a new approach using Monte Carlo (MC) simulations of the electronic relaxation processes was presented.²³ In this method independent Brownian rotational trajectories of Gd³⁺ complexes are generated in discrete time steps. Similar numerical approaches had already been used in the past (for example in the work of Abernathy and Sharp²⁴), but in our case the simulated Hamiltonian took into account all contributions (static and transient) to the relaxation process. A MC procedure for the reorientation of the Gd³⁺ complexes, combined with an Ornstein–Uhlenbeck process^{25,26} used to model the transient zero-field splitting, was applied to the electronic relaxation theory beyond the Redfield limit where there is no analytical solution. A comparison of the simulation results with the Redfield predictions allowed a rigorous estimation of the error induced by the Redfield approximation outside its limits. The slow molecular tumbling at low temperature was found to be of no consequence for the relatively small studied complexes ([Gd(H₂O)₈]³⁺ and [Gd(DOTA)(H₂O)]⁻) in the range of conventional EPR (0.34 T and above), but the extrapolation of the Redfield theory down to low fields (0.1 T and below) led to significant discrepancies. For example, the simulated electronic relaxation times were over 20% longer than the Redfield predictions for the aqua ion. This was an important finding since such low magnetic fields are routinely used in NMRD experiments on Gd³⁺ complexes.

Although this improved theory has brought new insights into the phenomena underlying electron spin relaxation, it has also dug an increasingly wide gap between the ¹H/¹⁷O NMR experiments commonly performed in the study of potential MRI contrast agents and the state of the art in the field of EPR. In particular, the simultaneous fitting approach first proposed by Powell et al.⁴ has become arguable at best. In this paper, we present, for the first time, an integrated and theoretically sound approach combining ¹⁷O NMR, NMRD, and EPR experimental data with a full description of electron spin relaxation, taking possible violations of Redfield's approximation into account. The selected test case is the octa aqua ion [Gd(H₂O)₈]³⁺. We

(9) Gonzalez, G.; Powell, D. H.; Tissières, V.; Merbach, A. E. *J. Phys. Chem.* **1994**, *98*, 53–59.
 (10) Poupko, R.; Baram, A.; Luz, Z. *Mol. Phys.* **1974**, *27*, 1345–1357.
 (11) Strandberg, E.; Westlund, P.-O. *J. Magn. Reson.* **1999**, *137*, 333–344.
 (12) Smirnova, T. I.; Smirnov, A. I.; Belford, R. L.; Clarkson, R. B. *J. Am. Chem. Soc.* **1998**, *120*, 5060–5072.
 (13) Redfield, A. G. *The Theory of Relaxation Processes*; Redfield, A. G., Ed.; Academic Press Inc: New York, 1965; Vol. 1, pp 1–32.
 (14) Rast, S.; Fries, P. H.; Belorizky, E. *J. Chim. Phys.* **1999**, *96*, 1543–1550.
 (15) Rast, S.; Fries, P. H.; Belorizky, E. *J. Chem. Phys.* **2000**, *113*, 8724–8735.
 (16) Rast, S.; Borel, A.; Helm, L.; Belorizky, E.; Fries, P. H.; Merbach, A. E. *J. Am. Chem. Soc.* **2001**, *123*, 2637–2644.
 (17) Micskei, K.; Powell, D. H.; Helm, L.; Brücher, E.; Merbach, A. E. *Magn. Reson. Chem.* **1993**, *31*, 1011–1020.
 (18) Curl, R. F. *J. Mol. Phys.* **1965**, *9*, 585–597.
 (19) Nyberg, G. *Mol. Phys.* **1967**, *12*, 69–81.
 (20) Rast, S.; Belorizky, E.; Fries, P. H.; Travers, J. P. *J. Phys. Chem. B* **2001**, *105*, 1978–1983.

(21) Abragam, A. *The Principles of Nuclear Magnetism*; Oxford University Press: London, 1961.
 (22) Abragam, A., Ed.; Oxford University Press: London, 1961; pp 281–283.
 (23) Rast, S.; Fries, P. H.; Belorizky, E.; Borel, A.; Helm, L.; Merbach, A. E. *J. Chem. Phys.* **2001**, *115*, 7554–7563.
 (24) Abernathy, S. M.; Sharp, R. R. *J. Chem. Phys.* **1997**, *106*, 9032–9043.
 (25) Kannan, D. *An Introduction to Stochastic Processes*; Elsevier North-Holland: New York, 1979.
 (26) Bauer, H., Ed.; de Gruyter: Berlin, 1991; pp 259–267.

discuss the physical relevance of the calculated parameters and compare our values with those obtained in earlier papers. We also consider the practical usability of our approach and discuss the impact of our new theoretical framework on future experimental studies.

Theoretical Section

Since most of the theory has already been presented in earlier papers, we will only present here the parts where the general approach of Powell et al.^{1,4} must be modified to include Rast's approach of the electron spin relaxation.^{13–15,22}

Time Correlation Functions. NMR time correlation functions in the absence of cross-relaxation can be written as a product of the time correlation functions for the various active relaxation mechanisms (eq 1).²⁷

$$g(t) = g_a(t)g_b(t)\cdots g_x(t) \quad (1)$$

The 1D NMR line shape is simply the Fourier transform of the overall time correlation function (eq 2)

$$I(\omega) = \int_0^\infty e^{-i\omega t} g(t) dt \quad (2)$$

In the case of solutions of paramagnetic agents, this leads eventually to the well-known equations of Solomon–Bloembergen^{28,29} and Freed^{30,31} for ¹H relaxation and to the Swift–Connick³² equations for ¹⁷O.

Whereas it is observed that the longitudinal relaxation can be adequately described by a single correlation time T_{1e} ^{14–16} (i.e. $g_{ze}(t) = \exp(-t/T_{1e})$), the transverse relaxation function of $S = 7/2$ ions is generally a combination of four time correlation functions with different intensities I_k and characteristic times T_{2ek} , $k = 1–4$ (eq 3)

$$g_{xe}(t) = \sum_{k=1}^4 I_k \exp(-t/T_{2ek}) \quad (3)$$

Consequently, this multiexponential behavior should be reflected in all equations where transverse electronic relaxation plays a role.

Outer-Sphere Relaxivity. As found by Freed,³¹ the spectral density for dipolar relaxation modulated by free diffusion and finite electronic relaxation is given by eq 4

$$J_n(\omega) = 2 \operatorname{Re} \int_0^\infty G(t) \exp([-i\omega + 1/T_{ne}]t) dt, \quad n = 1, 2 \quad (4)$$

where $G(t)$ is the time correlation function obtained from the solution of Smoluchowski's diffusion equation. If we now substitute the electronic decaying exponential with our expression of $g_{xe}(t)$ (eq 3), we obtain the correct form of $J_2(\omega)$ (eq 5)

$$J_2(\omega) = 2 \operatorname{Re} \int_0^\infty G(t) g_{xe}(t) \exp(-i\omega t) dt = \\ 2 \sum_{k=1}^4 \operatorname{Re} I_k \int_0^\infty G(t) \exp([-i\omega + 1/T_{2ek}]t) dt = \\ \sum_{k=1}^4 I_k J_{2, \text{Freed}}(\omega, T_{2ek}) \quad (5)$$

Thus we see that the effect of a multiexponential electronic relaxation is only to replace the single T_{2e} -dependent spectral density with a linear combination of individual spectral densities with respective coefficients I_k , $k = 1–4$. Incidentally, the effect of the dynamic frequency shift (imaginary part of T_{2ek}) is negligible as it is always small compared to the electronic frequency ω used for J_2 .

Inner-Sphere Relaxivity and ¹⁷O Longitudinal Relaxation. Both ¹H and ¹⁷O inner-sphere longitudinal dipolar relaxation rates depend on the transverse electronic relaxation through the second dipolar correlation time τ_{d2} defined by eq 6

$$\frac{1}{\tau_{d2}} = \frac{1}{\tau_m} + \frac{1}{\tau_R} + \frac{1}{T_{2e}} \quad (6)$$

This definition expresses the relative independence of the chemical exchange, molecular rotation, and electronic relaxation processes that modulate the dipolar interaction. Similar to the previous example, the corresponding spectral density must then be rewritten as eq 7

$$J_2(\omega) = \int_0^\infty g_M(t)g_R(t)g_{xe}(t) \exp(-i\omega t) dt = \\ \sum_{k=1}^4 I_k \int_0^\infty g_M(t)g_R(t) \exp([-i\omega + 1/T_{2ek}]t) dt = \\ \sum_{k=1}^4 I_k J_{2, \text{std}}(\omega, T_{2ek}) \quad (7)$$

However, one may question the independence of the relaxation mechanisms. Indeed, electronic relaxation is itself a function of rotational diffusion, which modulates the static crystal field in the laboratory frame. The consequences of this correlation are 2-fold:³³ (i) cross relaxation effects appear between the nuclear dipolar relaxation and the electron relaxation and (ii) cross terms also appear between the dipolar and scalar relaxation processes. We can overlook (i) since it only affects the transverse nuclear relaxation³⁴ and thus plays no role in our study of ¹H relaxation where only T_1 is considered. The second effect, arising from the artificial separation of the electron-nucleus coupling into two contributions, can also be neglected for the inner-sphere protons where scalar relaxation is negligible. For ¹⁷O, one should in principle take this effect into account. However, in our case it can be conveniently neglected, as it is only important when the time-dependent interaction (static crystal field) is stronger than the electron Zeeman interaction.^{35,36} In the conditions of ¹⁷O NMR (minimum external field 1.4 T

(27) Vigouroux, C.; Belorizky, E.; Fries, P. H. *Eur. Phys. J. D* **1999**, *5*, 243–255.

(28) Bloembergen, N. *J. Chem. Phys.* **1957**, *27*, 572–573, 595–596.

(29) Bloembergen, N.; Morgan, L. O. *J. Chem. Phys.* **1961**, *34*, 842–850.

(30) Hwang, L.-P.; Freed, J. H. *J. Chem. Phys.* **1975**, *63*, 4017–4025.

(31) Freed, J. H. *J. Chem. Phys.* **1978**, *68*, 4034–4037.

(32) Swift, T. J.; Connick, R. E. *J. Chem. Phys.* **1962**, *37*, 307–320.

(33) Kowalewski, J.; Nordenskiöld, L.; Benetis, N.; Westlund, P.-O. *Prog. NMR Spectrosc.* **1985**, *17*, 141–185.

(34) Benetis, N.; Kowalewski, J.; Nordenskiöld, L.; Wennerström, H.; Westlund, P.-O. *Mol. Phys.* **1983**, *50*, 515–530.

(35) Benetis, N.; Kowalewski, J.; Nordenskiöld, L.; Wennerström, H.; Westlund, P.-O. *Mol. Phys.* **1983**, *48*, 329–346.

(36) Benetis, N.; Kowalewski, J.; Nordenskiöld, L.; Wennerström, H.; Westlund, P.-O. *J. Magn. Reson.* **1984**, *58*, 261–284.

in our data), this is not the case for the Gd³⁺ aqua ion, nor for any of the polyaminocarboxylate complexes studied so far.^{15,16}

The same argument might be raised regarding chemical exchange (which modulates the crystal field tensor by changing the coordination sphere). This does not hold for Gd³⁺ complexes where chemical exchange is at least 2 orders of magnitude slower than electronic relaxation: we can safely assume a fixed coordination sphere (except for small vibrations) on the EPR time scale.

¹⁷O Transverse (Scalar) Relaxation. In a very similar manner, the scalar relaxation mechanism dominating the transverse relaxation of inner sphere ¹⁷O is influenced by T_{2e} through the second scalar correlation time τ_{2S} (eq 8)

$$\frac{1}{\tau_{2S}} = \frac{1}{\tau_m} + \frac{1}{T_{2e}} \quad (8)$$

The spectral densities should therefore be substituted accordingly, yielding eq 9

$$\frac{1}{T_{2sc}} = \frac{(A/\hbar)^2}{3} S(S+1) \left[\tau_{1S} + \sum_{k=1}^4 J_k \frac{\tau_{2Sk}}{1 + \omega^2 \tau_{2Sk}^2} \right] \quad (9)$$

There is no need to consider cross-relaxation effects in this case, since the dipolar contribution is negligible compared to the scalar term.

Low-Field NMRD and the Redfield Limit. Very recently, Rast et al.²³ studied the electronic relaxation correlation functions of [Gd(H₂O)₈]³⁺ and [Gd(DOTA)(H₂O)]⁻ beyond the Redfield limit using Monte Carlo simulations. The validity region of Redfield's theory is defined by the two following conditions regarding the time-dependent Hamiltonian H_1 and the associated correlation time τ_c (eqs 10 and 11).

$$|H_1| \tau_c \ll 1 \quad (10)$$

$$|H_1|^2 \tau_c \ll \omega_0 \quad (11)$$

Whereas condition (10) was found to play no significant role for the studied complexes even when it was not properly fulfilled,²³ condition (11) can be the source of significant discrepancies at low magnetic fields (0.1 T and below). For the octa aqua ion, MC calculations using the parameters obtained by simultaneous fitting of multiple temperature and frequency EPR spectra led to low-field electronic relaxation times over 30% longer than the Redfield predictions (see Figure 1). At higher fields, the MC prediction converges with the Redfield approximation. The Redfield limit violation is especially problematic when NMRD profiles are considered. The lowest magnetic fields in these experiments are on the order of 10⁻³ Tesla, and electronic relaxation plays an important role in the low-field region of the profile. For large complexes, it even becomes the dominant term in the dipolar correlation time τ_d as rotational diffusion slows down.

Since Redfield's theory breaks down at low fields, one should not expect to obtain an agreement between the electronic parameters derived from a complete EPR line shape analysis and those derived from the NMRD profile using the standard Solomon–Bloembergen–Morgan equations.²⁹ Worse, the determination of the electronic parameters by the low-field relaxivity alone using a Redfield approach can lead to erroneous

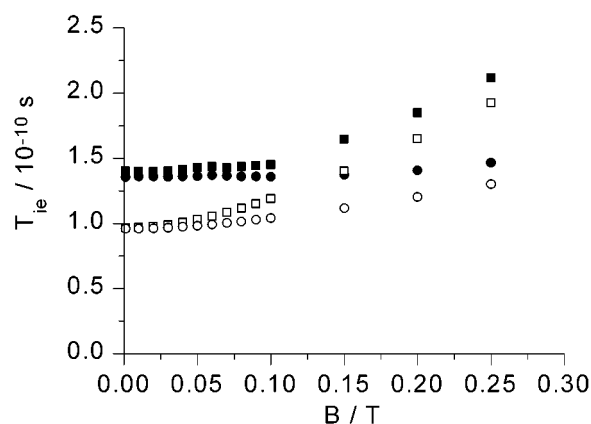


Figure 1. Longitudinal (squares) and transverse (circles) electronic relaxation times of an $S = 7/2$ spin using parameters from ref 16 from MC simulations (full symbols) and Redfield's theory (empty symbols)

results irrelevant at higher fields (typical medical magnetic resonance imaging fields, ¹⁷O NMR, or EPR).

The Monte Carlo (MC) approach presented recently²³ allows a numerical calculation of the electronic spin time correlation functions even out of the Redfield validity region. To take advantage of the information provided by the low-field part of the NMRD profile, one should perform a MC simulation for each NMRD data point. However, the computational cost of such a calculation would be prohibitive. Therefore we propose a mixed approach. For relaxivity measurements above a safe limit (say 0.1 T), one is allowed to use a Redfield description of the electronic relaxation. At a low enough field (below 0.01 T) the NMRD profile is essentially flat and can be approximated by fitting only one average value with an appropriate statistical weight.

Simultaneous Fitting of EPR, ¹⁷O NMR, ¹H NMR, and Low-Field NMRD. We performed a nonlinear least-squares fitting of the modified standard model against the extensive variable temperature data^{4,6} available about the Gd³⁺ octa aqua ion. New multiple temperature NMRD profile were recorded. Freshly prepared Gd(ClO₄)₃ was dissolved in bidistilled water to obtain a 1.34 mM solution. Multiple temperature measurements were performed on this sample using a Stellar fast field-cycling relaxometer. The initial parameters in the fitting procedure were those of Powell et al.⁴ (see Table 1) except for the following: the Gd–H relative diffusion constant was fixed to the sum of the water ($22.36 \times 10^{10} \text{ m}^2/\text{s}$ ³⁷) and aqua ion ($3.9 \times 10^{10} \text{ m}^2/\text{s}$ ³⁸) self-diffusion coefficients and the electronic parameters a_2 , a_4 , a_6 , a_{2T} , τ_v , and g of Rast et al.¹⁶ were used for the electronic part. The rotational correlation time τ_R was that of Powell (41 ps), while its activation energy was restrained to reasonable values (16–19 kJ/mol) as discussed by Rast based on the temperature dependence of water viscosity. Note that τ_R reported in this paper is the second-order correlation time $\tau_2 = 1/(6 \times D_R)$ relevant for NMR. This convention is rather arbitrary from the EPR point of view, since the fourth ($\tau_4 = 1/(20 \times D_R)$) and sixth order ($\tau_6 = 1/(42 \times D_R)$) correlation times are also used. However it allows an easier comparison with earlier simultaneous fitting studies such as Powell's. In general, care should be taken not to confuse the NMR definition ($\tau_R = \tau_2$)

(37) *Handbook of Chemistry and Physics*, 67 ed.; CRC Press: Boca Raton, FL, 1986.

(38) Vigouroux, C.; Bardet, M.; Belorizky, E.; Fries, P. H.; Guillermo, A. *Chem. Phys. Lett.* **1998**, 93–100.

Table 1. Parameters Obtained through Simultaneous Fitting of EPR, ^{17}O NMR, and NMRD Data. Underlined Values Were Either Fixed or Have Reached Their Imposed Limit

	this work	NMR/EPR ^a	EPR ^b
ΔH^\ddagger [kJ/mol]	18.2 ± 5	15.3	
$k_{\text{ex}298}$ [10^6 s^{-1}]	682 ± 140	804	
E_{R} [kJ/mol]	19	15.0	18.9
τ_{R}^{298} [ps]	35.3 ± 1	41	23.3
E_{v} [kJ/mol]	14.9 ± 2		9.2
τ_{v}^{298} [ps]	1.05 ± 0.3		0.63
A/\hbar [10^6 rad/s]	-5.21 ± 0.04	-5.3	
D_{GdH}^{298} [$10^{-10} \text{ m}^2 \text{ s}^{-1}$]	26	23	
E_{DGdH} [kJ/mol]	22	22	
Gd–O [Å]	2.5	2.5	
Gd–H [Å]	3.05	3.1	
$\chi(1 + \eta^2/3)^{1/2}$ [MHz]	6.12 ± 1.4	7.58	
g	1.993	2	1.99273
a_2 [10^{10} s^{-1}]	0.0946 ± 0.14		0.38
a_4 [10^{10} s^{-1}]	0		0.024
a_6 [10^{10} s^{-1}]	0.0232 ± 0.003		0.021
$a_{2\text{T}}$ [10^{10} s^{-1}]	0.687 ± 0.04		0.65

^a Reference 4. ^b Reference 16.

and the more general, six times longer rotational diffusion correlation time ($\tau_{\text{R}} = 1/D_{\text{R}}$).

The 14 free parameters in the model (room-temperature water exchange rate k_{ex}^{298} , activation enthalpy ΔH^\ddagger , rotational correlation time τ_{R} and associated activation energy E_{R} , transient zero-field splitting correlation time τ_{v} and associated activation energy E_{v} , ^{17}O scalar coupling constant A/\hbar , ^{17}O quadrupolar coupling constant $\chi(1 + \eta^2/3)^{1/2}$, activation energy for the relative ^1H – Gd^{3+} diffusion E_{DGdH} , Gd^{3+} electronic g factor, static (a_2 , a_4 , a_6) and transient ($a_{2\text{T}}$) crystal field parameters) were simultaneously adjusted to the multiple temperature and magnetic field/frequency data (^{17}O NMR $1/T_1$, $1/T_2$, and chemical shifts, EPR peak-to-peak width and resonance field, ^1H NMRD above 10 MHz and an averaged low frequency point at 0.141 MHz). For the analysis of ^1H NMRD, we fixed the inner-sphere Gd–H distance to 3.05 Å instead of 3.1 Å. This shorter value was evaluated as the average between the experimental Sm–D (3.11 Å) and Dy–D (3.03 Å) obtained from neutron diffraction measurements, slightly biased toward the clearly 8-coordinated $[\text{Dy}(\text{H}_2\text{O})_8]^{3+}$ value.³⁹ We reverted to the use of reduced values (peak-to-peak width ΔH_{pp} and central field) instead of the full EPR spectra to simplify the parallel treatment of ^{17}O NMR and NMRD, although the analysis of the full line shape is in principle better.¹⁶ Since the deviation from the pure Lorentzian line shape was observed to be very small for $[\text{Gd}(\text{H}_2\text{O})_8]^{3+}$, the choice of method is mostly a matter of taste in this case.

The fit function was included in the more general program VISUALISEUR,⁴⁰ running on the MATLAB⁴¹ environment. We used FORTRAN subroutines derived from the EPR program from ref 16 for the calculation of the EPR peak to peak widths, center fields, and the electronic relaxation rates within the Redfield approximation. For low-frequency NMRD, the program described in ref 23 was used to simulate the longitudinal and transverse electron spin correlation functions, from which the effective relaxation time was extracted by a linear regression. To reduce the computation time, only 1000 time steps were used to generate the spin dynamics instead of 16000.²³ As shown

in Figure 1, this was sufficient to reproduce the relaxation times reported in the original paper and allowed the calculation of one low-field relaxivity value in 5 min on a workstation (Linux on a 700 MHz AMD Duron CPU).

Results and Discussion

The calculated parameters are reported in Table 1, together with the parameters obtained by Powell et al.⁴ The experimental results and theoretical curves are shown in Figure 2. The agreement between the experimental data and the simulated curves is very good, even for NMRD points between 1 and 10 MHz, which were not included in the fitting procedure.

In general, we observe that the parameters specific to NMR are left rather unchanged by the new model of EPR relaxation. The water exchange rate is somewhat decreased compared to the work of Powell, but within the calculated standard error. The exchange activation enthalpy is also similar to the earlier value. The scalar coupling constant is mostly unaffected by the simultaneous adjustment, since it is essentially determined by the ^{17}O chemical shifts. As discussed by Powell et al., the calculated quadrupolar coupling constant is very sensitive to the choice of the Gd–O distance so only one of these parameters should be considered adjustable. By fixing the Gd–O distance to 2.5 Å, they obtained a coupling constant of 2.0 ± 2.3 MHz (compared to 7.58 MHz for acidified water), whereas fixing the coupling constant to 7.58 yielded a Gd–O distance of 2.76 Å. Since the distance has been determined both by experimental⁴² and theoretical methods^{43,44} to be in the 2.4–2.6 Å region, we preferred to use the fixed 2.5 Å value. Our result for $\chi(1 + \eta^2/3)^{1/2}$ is 6.12 ± 1.38 MHz and thus closer to the value for free water. It is useful to compare this value to the one determined by Leyte and co-workers⁴⁵ for ^{17}O in the first coordination shell of Mg^{2+} ($\chi = 5.7 \pm 0.3$ MHz, $\eta = 0.93$). A rough estimation based on the ratio of the radial electric field gradients ($\text{Mg}^{2+}\text{--O} \approx 2.1$ Å, $\text{Gd}^{3+}\text{--O} \approx 2.5$ Å) yields $\chi(\text{Gd--O})/\chi(\text{Mg--O}) = 0.889$ or $\chi(\text{Gd--O}) = 5.1$ MHz. Using the same asymmetry parameter, we obtain for $[\text{Gd}(\text{H}_2\text{O})_8]^{3+}$ the estimation that $\chi(1 + \eta^2/3)^{1/2} = 5.8$ MHz, in very good agreement with our result.

Since the influence of the rotational correlation time on the electron spin relaxation is part of the new theory, it is not surprising that the adjusted value should change compared with those of the earlier studies. Indeed the rotation and the electron spin relaxation are highly correlated in our simultaneous fitting approach, since the dipolar correlation time dominating the low-field relaxivity is simply the reciprocal sum of the electron spin relaxation time and the rotational correlation time (see eq 6). Therefore, the fitting procedure imposes rather strict constraints on this parameter, even more so since we have set boundaries compatible with the temperature dependence of the viscosity of water for the activation energy. The value we obtain (35.3 ± 1.0 ps) is certainly compatible with the estimations based on the Stokes Einstein relation (22 ps if a microviscosity correction factor is included, 53 ps if it is not¹⁵).

The change in the rotation correlation time is reflected by a change in the crystal field parameters compared with the EPR-

(39) Cossy, C.; Helm, L.; Powell, D. H.; Merbach, A. E. *New J. Chem.* **1995**, 27–35.

(40) Yerly, F. *VISUALISEUR* 2.3.1: Lausanne, 2001.

(41) *MATLAB* 6.0.0.88; The Mathworks, Inc., 2000.

(42) Kurisaki, T.; Yamaguchi, T.; Wakita, H. *J. Alloys Compd.* **1993**, 192, 293–295.

(43) Hengrasme, S.; Probst, M. M. *Z. Naturforsch.* **1991**, 46a, 117.

(44) Schäfer, O.; Daul, C. *Int. J. Quantum Chem.* **1997**, 61, 541–546.

(45) Struis, R. P. W. J.; de Bleijser, J.; Leyte, J. C. *J. Phys. Chem.* **1987**, 91, 6309–6315.

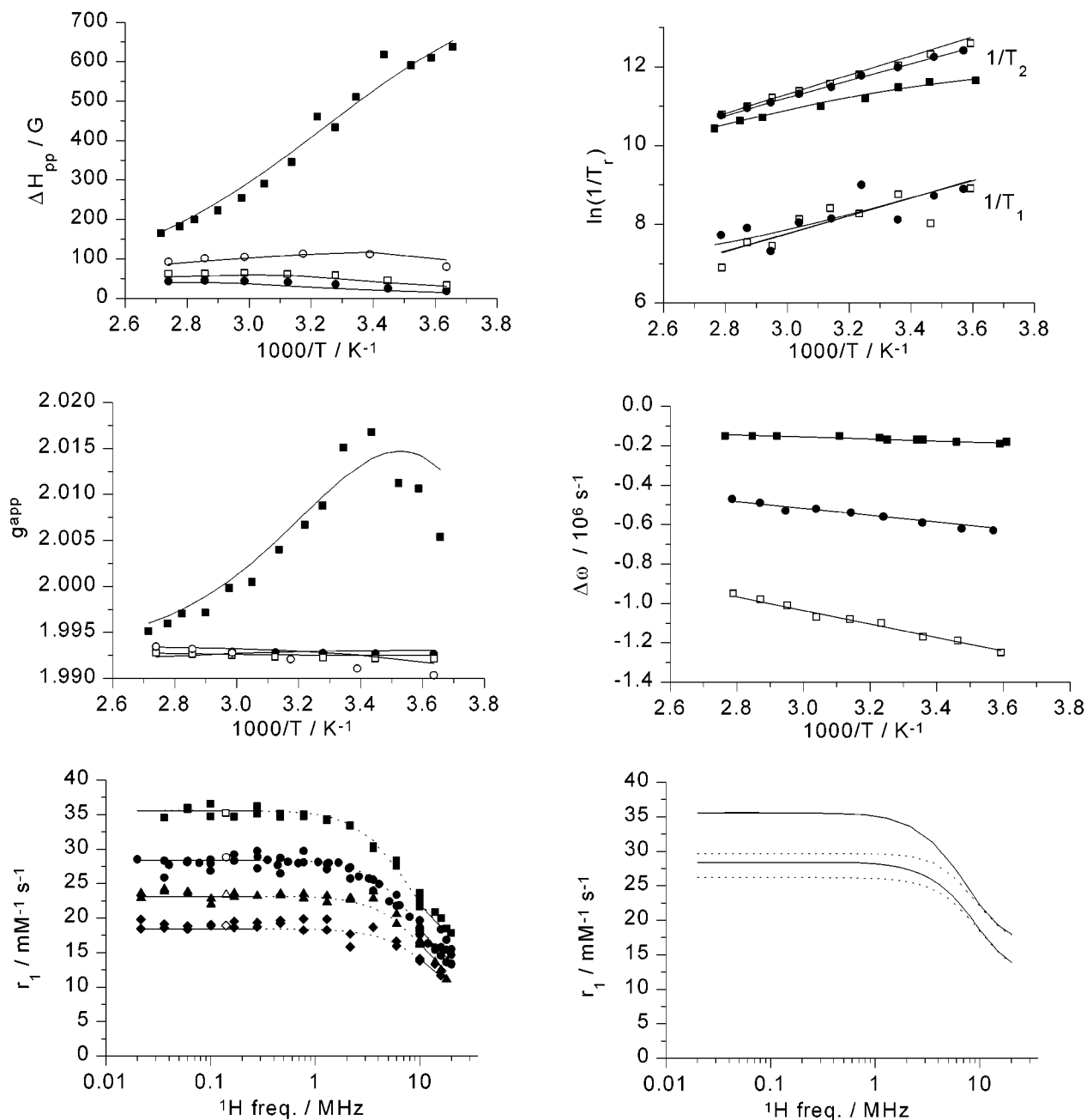


Figure 2. EPR peak-to-peak width and apparent *g*-factor at X-band (squares), 75 GHz (triangles), 150 GHz (diamonds) and 225 GHz (circles); reduced ¹⁷O relaxation rates and chemical shifts at 1.41 T (□), 4.7 T (●) and 9.4 T (■). NMRD profiles at 283.2 K (■), 298.2 K (●), 310.4 K (▲), 323.0 K (◆), with the empty symbols corresponding to averaged values over the low-field part of the profile; comparison with the predictions of Redfield's theory using the same electronic parameters at 10 °C and room temperature (dotted lines).

only analysis. In turn, this affects the Gd³⁺ *g* factor since this parameter is essentially determined by the EPR resonance field, where the electron spin relaxation induces dynamic frequency shifts.^{10,46} On the basis of earlier studies in the solid⁴⁷ and in solution,¹⁶ we set an upper boundary of 1.9930 for *g*. Even if the calculated value has hit this limit, the final adjustment is very good as can be seen from temperature and spectrometer frequency dependence of the apparent *g* factor, *g*^{app} (Figure 2).

The transient zero-field splitting parameters *a*_{2T}, *τ*_v, and *E*_v are very close to those obtained through EPR only. Thus their effect on the EPR line shape (negligible at X-band, increasing

contribution at higher frequencies) is essentially the same. This means that the crystal field parameters obtained by solution EPR only are not very precisely determined. In particular, error compensation between the 5 parameters in question (*a*₂, *a*₄, *a*₆, *τ*_R, *E*_R) during the fit seems to be a serious problem that could be solved through the use of independent constraints (based either on NMR or solid-state EPR or maybe on some future developments regarding the direct determination of *T*_{1e}⁴⁸).

The total crystal field splitting of the ⁸S multiplet can be calculated thanks to the *D*_{4d} symmetry of the [Gd(H₂O)₈]³⁺ complex.¹⁵ The crystal field Hamiltonian reduces to eq 12

$$\hat{H} = \sum_{k=2,4,6} B_k \hat{T}_0^k \quad (12)$$

(46) Fraenkel, G. K. *J. Chem. Phys.* **1965**, *42*, 4275–4298.
 (47) Abragam, A., Bleaney, B., Eds.; Oxford University Press: Oxford, 1970; pp 335–339.

where \hat{T}_0^k is an irreducible tensor of order k^{49} and the coefficients B_k are such that $a_k = |B_k|$. With our parameters, the fourth-order contribution vanishes, so there are only two possible combinations. Either B_2 and B_6 have the same sign, with a total splitting of 0.37 cm^{-1} , or their sign is different and the splitting is 0.38 cm^{-1} . One of the terms is obviously dominant, and indeed we find that the sixth-order contribution alone leads to a splitting of 0.36 cm^{-1} . It is somewhat strange that the highest order term should contribute so much to the effect. There may be some compensation between the various orders, as it has been noted in earlier studies.¹⁶ Nevertheless the overall value is in reasonable agreement with the available direct experimental measurements (0.25 cm^{-1} for Gd^{3+} in a solid lanthanum ethyl sulfate matrix⁴⁷).

Using our parameters, the low-field limit of the electron relaxation time in the Redfield approximation is 89 ps at 298 K for both T_{1e} and T_{2e} and 60 ps at 283 K. The MC simulation yields longer values, with $T_{1e} = 122 \text{ ps}$, $T_{2e} = 117 \text{ ps}$ at room temperature and $T_{1e} = 95 \text{ ps}$, $T_{2e} = 90 \text{ ps}$ at 283 K. These small apparent differences between T_{1e} and T_{2e} can be explained by numerical errors. The Redfield error can thus be estimated to 25% at room temperature (similar to the result calculated from the parameter set obtained by EPR only²³) and 36% at 283 K. In the NMRD profile, at low field ($< 1 \text{ MHz}$), τ_R and $T_{1,2e}$ are strongly correlated. Since τ_R is usually well-known from ^{17}O and ^1H NMR experiments at higher fields, it is tempting to obtain microscopic electron spin parameters (τ_{S0} , Δ^2 , or a_k and the respective correlation times depending on the model) based on these measurements. However, to extract either of these quantities using a simple Solomon–Bloembergen–Morgan-like approach of the electron spin relaxation will probably yield results irrelevant at higher magnetic fields where the Redfield theory becomes applicable. Since the influence of $T_{1,2e}$ on NMR decreases at higher fields (rotation becoming the dominant term for dipolar relaxation), it is quite conceivable to obtain in this fashion electron spin parameters compatible with ^{17}O NMR and NMRD but fail to describe EPR experiments.

Conclusion

The recent development of an improved theory of the EPR of Gd^{3+} complexes in solution is an important step toward understanding the influence of molecular structure on the electron spin relaxation. This theory has been used successfully to analyze the EPR spectra of a number of complexes, but its

consequences on ^1H and ^{17}O NMR were still unclear. Using the latest refinements, we have shown for the first time that a rigorous simultaneous analysis of EPR, ^{17}O NMR, and NMRD experiments performed on Gd^{3+} complexes in solution is feasible and demonstrated the approach using the extensive data available on the $[\text{Gd}(\text{H}_2\text{O})_8]^{3+}$ aqua ion. After an elaborate fitting procedure, quite manageable with today's computational power, we were able to reproduce the experimental data with a very good quality of fit. The better understanding of the electron spin relaxation obtained through the recent EPR studies allowed us to fix several parameters to physically reasonable values, decreasing the number of degrees of freedom of our statistical system. All the values we calculate for the adjustable parameters can be analyzed from the point of view of their physical meaning, and we found them to be satisfactory.

The simultaneous analysis was again found to remove some of the statistical problems due to the interdependence of some parameters. Different experiments impose different constraints on the parameters, allowing a better determination of their values.

The results cast a doubt on the usefulness of low-field NMRD as an experimental technique in the field of Gd^{3+} contrast agents. Indeed the larger part of the NMRD profile (^1H frequency $< 1 \text{ MHz}$) can only be used to extract the low-field dipolar correlation time τ_d , the reciprocal sum of the rotation correlation time τ_R and the low-field electron spin relaxation time (sometimes noted as τ_{S0}). Since the Redfield limit is violated for the Gd^{3+} electron spin at such low magnetic fields, the transferability of the electron spin parameters obtained in this fashion to higher fields (among which the typical medical imaging conditions, ^1H frequency = 20–60 MHz) is a difficult problem in the simplest case (for example the octa aqua ion). In other words, larger molecules (such as typical real-life MRI contrast agents) require the full extent of the newer theory (not limited by Redfield's approximations) for a rigorous analysis of the complete NMRD profile.

Acknowledgment. We are appreciative of the Swiss National Science Foundation and the Office for Education and Science (OFES) for their financial support. This research was carried out in under the EC COST Action D-18 Lanthanide Chemistry for Diagnosis and Therapy.

Supporting Information Available: Multiple temperature NMRD profiles described in the experimental section are given in table S1 (PDF). This material is available free of charge via the Internet at <http://pubs.acs.org>.

JA016919F

(48) Atsarkin, V. A.; Demidov, V. V.; Vasneva, G. A. *Phys. Rev. B* **1995**, *52*, 1290–1296.

(49) Buckmaster, H. A.; Chatterjee, R.; Shing, Y. H. *Phys. Stat. Sol. (a)* **1972**, *13*, 9–50.